Scuola IMT Alti Studi Lucca

Unveiling the relation between aesthetic experiences and attention through a cross-experiment validation of their processing biomarkers

Questa è la versione sottoposta a revisione paritaria (postprint) della seguente opera:

Original
Unveiling the relation between aesthetic experiences and attention through a cross-experiment validation of their processing biomarkers / Barbieri, Paolo; Berto, Martina; Sarasso, Pietro; Frascaroli, Jacopo; Handjaras, Giacomo; Piovesan, Francesca; Gnecco, Giorgio Stefano; Bottari, Davide; Ronga, Irene. - In: PNAS NEXUS. - ISSN 2752-6542. - (2025). [10.1093/pnasnexus/pgaf288]

Availability:
This version is available at: 20.500.11771/36078

Publisher:

Published
DOI:10.1093/pnasnexus/pgaf288

Terms of use:

This publication is made accessible in accordance with the terms for deposit in the institutional repository, as defined by the IMT School for Advanced Studies Lucca’s Open Access Policy. (https://library.imtlucca.it/sites/default/files/regolamento-policy-open-access-imtlib_0.pdf).

Si prega di consultare le pagine informative dell'editore relative alle politiche di autoarchiviazione.

(Article begins on next page)

02 May 2026

Unveiling the relation between aesthetic experiences and attention through a cross-experiment validation of their processing biomarkers

Paolo Barbieri[1], Martina Berto[2], Pietro Sarasso[1], Jacopo Frascaroli[1], Giacomo Handjaras[2], Francesca Piovesan[1], Giorgio Gnecco[3], Davide Bottari[2], Irene Ronga[1]**

*These authors equally contributed to the present manuscript

1 *BIP (BraIn Plasticity and behaviour changes) Research Group, Department of Psychology, University of Turin, Italy.*
2 *Molecular Mind Lab, IMT School for Advanced Studies Lucca, Lucca, Italy.*
3 *AXES Research Unit, IMT School for Advanced Studies Lucca, Lucca, Italy.*

Corresponding author:

Irene Ronga
Department of Psychology, University of Turin
Via Verdi 10, 10124 Turin, Italy
Phone: +39 011 6703070
Fax: +39 011 8159039
E-mail: irene.ronga@unito.it

ACCEPTED MANUSCRIPT

Downloaded from https://academic.oup.com/pnasnexus/advance-article/doi/10.1093/pnasnexus/pgaf288/8249480 by guest on 16 September 2025

© The Author(s) 2025. Published by Oxford University Press on behalf of National Academy of Sciences. This is an Open Access article distributed under the terms of the Creative Commons Attribution-NonCommercial License (https://creativecommons.org/licenses/by-nc/4.0/), which permits non-commercial re-use, distribution, and reproduction in any medium, provided the original work is properly cited. For commercial re-use, please contact reprints@oup.com for reprints and translation rights for reprints. All other permissions can be obtained through our RightsLink service via the Permissions link on the article page on our site—for further information please contact journals.permissions@oup.com.

Author contributions

PB: Conceptualization; Data curation; Formal analysis; Investigation; Methodology; Writing-original draft; Writing-review and editing; **MB**: Data curation; Formal analysis; Investigation; Methodology; Writing-original draft; Writing-review and editing; **PS**: Conceptualization; Data curation; Formal analysis; Supervision; Investigation; Methodology; Writing-original draft; Writing-review and editing; **JF**: Conceptualization; Supervision; Funding acquisition; Writing-original draft; Writing-review and editing; **GH**: Conceptualization; Formal analysis; Methodology; Writing-review and editing; **FP**: Data curation; Investigation; Writing-original draft; **GG**: Conceptualization; Formal analysis; Supervision; Methodology; Writing-original draft; Writing-review and editing; **DB**: Conceptualization; Formal analysis; Supervision, Funding acquisition; Methodology; Writing-original draft; Writing-review and editing; **IR**: Conceptualization; Data curation; Supervision, Funding acquisition; Investigation, Methodology; Writing-original draft; Writing-review and editing.

Competing interests statement

The authors declare no competing interests.

Classification

Cognitive Neuroscience, Psychology.

Keywords

Neuroaesthetics; Aesthetic attitude; Attention; Event Related Potential (ERP); Machine learning

Data availability statement

Raw data collected in the pilot study and in Experiment 1 and 2 are fully available at these links (Mendeley: https://data.mendeley.com/preview/rp7r2xhhp9?a=1fb49ba5-88c0-4f6f-8539-4c3f781511ed; OSF: https://osf.io/uzh8r/). All codes employed to analyse pilot and Experiment 1 and 2 data are available for reviewers at these links (Mendeley:

ACCEPTED MANUSCRIPT

Downloaded from https://academic.oup.com/pnasnexus/advance-article/doi/10.1093/pnasnexus/pgaf288/8249480 by guest on 16 September 2025

https://data.mendeley.com/preview/rp7r2xhhp9?a=1fb49ba5-88c0-4f6f-8539-4c3f781511ed; OSF: https://osf.io/uzh8r/). The approved protocol for Stage 1 is available at this link (OSF, https://osf.io/uzh8r/).

Abstract

A centuries-old tradition encompassing philosophy, psychology and artistic practice describes aesthetic experiences as characterised by a special state of heightened attention towards external stimuli (i.e., an "aesthetic attitude"). In recent years, this view has motivated wide-ranging claims about the nature of our aesthetic encounters and the cognitive benefits of exposure to art. Despite sustained efforts from a growing stream of interdisciplinary research, however, it is still unclear whether aesthetic experiences can be systematically linked to observable attentional enhancements. In this study we address this long-standing question using electroencephalography and advanced machine learning techniques. We performed a series of EEG experiments measuring brain activity elicited by synthetic and natural images during an aesthetic (beauty judgements) and a pragmatic (symmetry judgements) task. Visual-evoked potentials and neural oscillations were used to assess whether the aesthetic tasks induce attentional enhancements. In line with our hypotheses, the power of alpha and beta pre-stimulus oscillations significantly decreased in the aesthetic *vs* pragmatic task. Furthermore, larger Late Positive Potential and N170 (the latter for natural images only) were found in the aesthetic *vs* pragmatic task. Accordingly, machine learning analyses demonstrated that pre-stimulus neural oscillations and N170 were systematically able to predict the type of task. Overall, our results highlight the presence of a perceptual processing enhancement and a heightened state of attention in aesthetic contexts. The upshot is a clearer understanding of the dynamics and neural underpinnings of our aesthetic experiences.

ACCEPTED MANUSCRIPT

Downloaded from https://academic.oup.com/pnasnexus/advance-article/doi/10.1093/pnasnexus/pgaf288/8249480 by guest on 16 September 2025

Significance statement

Our study addresses a question that has haunted scholars for centuries: Do experiences of beauty make us more focused on the world around us? By looking at the neural correlates of attention in an aesthetic *vs* a pragmatic task (judging the beauty vs the symmetry of visual stimuli), we detected neural indexes of amplified attention in the former. Through machine learning, we demonstrated that the tasks were distinguishable based on EEG features, corroborating our results. By revealing a systematic attentional enhancement in aesthetic tasks, our findings might have a transformative impact on all contexts in which individuals could benefit from better employment of their attentional resources, such as learning, rehabilitation, psychotherapy, and the promotion of adaptation in times of distress.

Introduction

A centuries-old tradition encompassing philosophy, psychology and artistic practice describes our experiences of beauty in art and nature as characterised by a special state of heightened attention towards external stimuli (i.e., an "aesthetic attitude", as some have called it)[1]. In philosophy, this idea is common currency at least since Kant, who describes judgements of taste as involving the careful engagement with the formal features of an object, with the sole purpose of prolonging its contemplation[2–4]. In line with this view, a recent strand of research suggests that aesthetic experiences demand high levels of attentional and working memory capacities, providing further support for the link between aesthetic appreciation and a heightened deployment of our attentional resources[5,6]. Previous neuroimaging studies have also indicated that aesthetic appreciation often corresponds to an increased activity along the neural perceptual hierarchy[7–10] similar to that underlying exogenous and endogenous attentional modulations [9–11]. Other neurophysiological studies found a magnification of well-established indexes of attentional amplification (i.e., the alpha event-related desynchronization – alpha ERD – and the early waves of the visual-evoked potentials – VEPs)[11,12] in subjects contemplating more appreciated abstract images[7].

ACCEPTED MANUSCRIPT

Downloaded from https://academic.oup.com/pnasnexus/advance-article/doi/10.1093/pnasnexus/pgaf288/8249480 by guest on 16 September 2025

So far, however, the attentional enhancement found in response to aesthetically appreciated stimuli has mainly been regarded as a bottom-up, transient effect produced by the features of the stimulus. There are however reasons to think that the same attentional enhancement can be prompted by top-down, task-related modulations [13]. In other words, the anticipation of having an aesthetic experience might have the same effects on our attention as having an aesthetic experience itself. Consistently with this latter hypothesis, in a series of fMRI studies, greater activations in visual areas were found when the same pictures were presented as artworks than when they were not [13]. Moreover, a series of EEG studies [14–16] found a difference in the late components of the ERP when participants were asked to make aesthetic (beautiful/not-beautiful) as opposed to descriptive (symmetric/not-symmetric) judgements about a set of geometric shapes, suggesting that there might be a functional dissociation of the neural processes involved in the two kinds of judgements (see also [17] for an FMRI study pointing in a similar direction). Differences in EEG responses (coinciding with the latency of the Late Positive Potential) were also found in a study where the subjects were asked to evaluate their liking as opposed to the correctness of the last chord of a sequence[18]. Importantly, however, while there are several studies examining whether aesthetic judgements might be underpinned by specific neural processes distinct from those involved in descriptive judgements, experimental studies designed to test whether aesthetic/evaluative tasks can systematically induce observable attentional enhancements are still lacking.

The present research fills this gap by comparing different electrophysiological indexes of attention, both pre-and post-stimulus and unfolding at different timescales, during an aesthetic *vs* a pragmatic evaluation task (see Figure 1). In Experiment 1, we asked participants to evaluate either the beauty (aesthetic task) or the symmetry (pragmatic task) of 180 abstract visual stimuli[10] containing different profiles of spectral frequency. In Experiment 2, the same participants evaluated the beauty or symmetry of 180 photos of real landscapes. Using synthetic and natural images, we aimed to test the generalizability of findings across different stimuli. During the task, we registered the EEG signal to compute pre-stimulus and post-stimulus attention-related indexes. More specifically, we analysed pre-stimulus alpha oscillations, post-stimulus alpha ERD and the early components of the VEP (expressed in the

ACCEPTED MANUSCRIPT

Downloaded from https://academic.oup.com/pnasnexus/advance-article/doi/10.1093/pnasnexus/pgaf288/8249480 by guest on 16 September 2025

first 200 ms following stimulus onset) to assess the presence of endogenous attentional processes associated with the aesthetic evaluation.

In this respect, we made two hypotheses (see Figure 2B and Table 1). If we could induce an "aesthetic attitude" (i.e., a top-down, tonic attentional enhancement during the aesthetic task as compared to the pragmatic task), we expected to observe in both experiments decreased pre-stimulus inhibitory alpha power and increased post-stimulus alpha ERD and VEP early components in the aesthetic task compared to the pragmatic one (Hypothesis 1). Furthermore, to validate and generalize findings, we used all relevant electrophysiological measures obtained in Experiment 1 (i.e., employing synthetic images), as biomarkers to classify whether participants were judging the beauty or the symmetry of natural images in Experiment 2. We hypothesized (Hypothesis 2) that the task (aesthetic vs pragmatic) performed on both natural and synthetic images could be distinguished based on electrophysiological signals both with high sensitivity and specificity.

Methods

Ethics information, sampling plan and pilot data

36 subjects with normal or corrected to normal vision participated in the study. Participants performed both Experiment 1 and 2 in two separate sessions (aesthetic and pragmatic) and in a randomized order, counterbalanced across participants. All participants gave their written informed consent to participate in the study, which complied with the guidelines required by the Declaration of Helsinki (2006) and was approved by the University ethics committee (Prot. n. 0433380 del 21/07/2023; University of Turin, Italy). The number of participants was estimated via simulations. We used the procedure described in Wang et al. [19] to simulate a dataset with two conditions (aesthetic and pragmatic) of VEP data, which are known to provide good SNR. First, based on the effects observed on the 5 subjects of a pilot study identical to Experiment 1, we selected 32 electrodes of interest at posterior locations (see section 2.1 of the Supplementary Information, from now on SI). For the simulation, we chose a time window

ACCEPTED MANUSCRIPT

Downloaded from https://academic.oup.com/pnasnexus/advance-article/doi/10.1093/pnasnexus/pgaf288/8249480 by guest on 16 September 2025

within the first 0.2s of the VEPs as it comprised both C1 and N170 waves [10]. The amplitude values at the electrodes of interest for the two conditions were sampled from a bivariate normal distribution (within-subject design) where mean and standard deviation were chosen based on the results of the five participants who performed the pilot study, (mean voltage aesthetic = 0.87; mean voltage pragmatic= 1.41; std aesthetic = 0.79; std pragmatic = 0.94). As hypothesized, participants collected in the pilot study showed a significant magnification of the early and middle-latency components of the VEP response (including C1 and N170 components) during the aesthetic compared to the pragmatic evaluation task. We then ran a cluster-based permutation on simulated datasets to test whether any statistical cluster (t-values) exhibited a significant difference between the two conditions with an alpha level of 0.05 (see section 2.2 of the SI for more details). The simulation results showed that to obtain power above 0.80 a sample size of N= 36 was required. The original algorithm used to perform such analyses can be downloaded from this link: https://osf.io/rmqhc/files/osfstorage.

If, during data collection, technical problems occured or registration was interrupted for any reason, we planned to discard the affected participants, and replace them with others to meet the required sample size (N = 36). Furthermore, a signal-to-noise ratio analysis was performed to discard noisy data. Specifically, we planned to exclude a participant's dataset if more than 30% of the epochs in one condition were marked for rejection (see the § Analysis Plan for details on the procedure). Details on EEG data analysis (including all the indications about artefact rejection) are included in the § Analysis Plan and SI. During the piloting phase, no participant was discarded.

Stimuli

In Experiment 1 we employed 180 2D black and white random noise images, with different profiles of spectral frequency, created with the IDL software (Harris Geospatial Inc. USA). All stimuli were generated with the same resolution (300 dpi), dimension (960x540), luminance and contrast (see also section 1.2 of the SI). In Figure 2A we show some examples of representative stimuli.

ACCEPTED MANUSCRIPT

Downloaded from https://academic.oup.com/pnasnexus/advance-article/doi/10.1093/pnasnexus/pgaf288/8249480 by guest on 16 September 2025

In Experiment 2 we employed 180 2D black and white photographs of natural landscapes (e.g. mountains, seashores). We chose images of natural landscapes for their ecological validity and because with this kind of stimuli judgements of symmetry and aesthetic appreciation seem to diverge more than with other stimulus categories [20]. We included a total of 180 stimuli homogenized for color spectrum (black and white), dimension, resolution, contrast and light reflection (see section 1.2 of the SI). Since some studies have shown that curved visual features generate a different response in the visual cortex compared to rectilinear stimuli [21] (something relevant to our examination of VEPs), stimuli in both sets were controlled for curvilinearity with the MLV Toolbox[22] (see SI for more details).

In Figure 2A we show five examples (2 from Experiment 1 and 3 from Experiment 2) of representative stimuli from the adjusted image set. Stimuli are available on Mendeley [doi: 10.17632/p4gp7xdmm7.1].

Experimental procedures

The setup and the procedures were identical for Experiments 1 and 2 and are represented in Figure 2B (please refer to sections 1.1 and 1.3 of the SI for further details on the apparatus). Participants sat at a table in a fixed position and were asked to look at and evaluate the abstract images (90 images, Experiment 1) or photographs (90 images, Experiment 2) presented on the screen while EEG data were recorded. Participants were presented with 2 different blocks (duration 40 minutes) for aesthetic and pragmatic evaluation and both the order of presentation of Experiment (synthetic and natural images) and Task (aesthetic and pragmatic evaluation) were randomized across participants. Visual stimuli were presented in a random order (stimulus duration 500 ms [23]), preceded by a cue (cue duration 500 ms [23]), preparing for the required evaluation. The experiment included a cue-stimulus delay period of 1 s [23]. A second delay period of 2 s followed the stimulus (see Figure 2B). A question mark then appeared on the blank screen, indicating to subjects that they should evaluate the beauty (during the aesthetic evaluation) or the symmetry (during the pragmatic evaluation) of the presented images on a 1 to 9 Likert scale [10,24] by pressing the corresponding numerical key on the computer keyboard. The evaluation scale ranged from 1 ('I completely dislike it' or 'it was

ACCEPTED MANUSCRIPT
Downloaded from https://academic.oup.com/pnasnexus/advance-article/doi/10.1093/pnasnexus/pgaf288/8249480 by guest on 16 September 2025

completely asymmetric') to 9 ('I like it very much' or 'it was very symmetric'). As soon as they responded, the next trial started.

Analysis plan

Electrophysiological recordings and preprocessing

EEG activity was recorded using 64 Ag-AgCl electrodes placed on the scalp of the participant according to the International 10-20 system and on-line referenced to FPz. Electrode impedances were kept below 5 kΩ. The electrooculogram (EOG) was recorded from two surface electrodes placed over the right below the lower eyelid and lateral to the outer canthus of the right eye. Signals were recorded and digitized by using a 64-channel EEG system BrainAmp DC (Brain Products Italia srl, Putignano, IT) with a sampling rate of 1000 Hz.

Processing pipeline and analysis strategy

The analysis was performed by implementing a previously validated pre-processing pipeline [25,26]. Raw EEG data were pre-processed with EEGLAB [27] (see section 3.1 of the SI). To detect stereotypical artifacts (eye movements, blinks, and heartbeat), we ran independent component analysis (ICA) [28] based on the extended Infomax [29,30]. Before computing ICA, data were lowpass filtered with a cut-off frequency of 40Hz (windowed sinc FIR filter, filter order 50), downsampled to 250Hz, and high pass filtered at 1Hz (windowed sinc FIR filter, filter order 500)[31]. ICA weights were then attributed to the original raw EEG (continuous and unfiltered signal with original sampling rate). The ICA procedure is fully described in the SI (section 3.2). The cleaned signal was lowpass filtered at 40 Hz (windowed sinc FIR filter, filter order 50), and downsampled to 250 Hz to reduce further computational time. A high pass filter of 0.1 Hz (windowed sinc FIR filter, filter order 5000) was applied to remove DC offset and slow drifts. In order to attenuate the 50Hz line noise artifact we used the Zapline-plus plugin [32,33]. Finally, noisy channels were interpolated using an automatic custom algorithm by Lalor (2009) [34] and Diliberto (2015; https://cnsp-workshop.github.io/website). Bad channels were rejected via spherical interpolation based on high or low threshold criteria; that is, a channel was marked

Downloaded from https://academic.oup.com/pnasnexus/advance-article/doi/10.1093/pnasnexus/pgaf288/8249480 by guest on 16 September 2025

ACCEPTED MANUSCRIPT

for rejection when its standard deviation was higher than three or lower than six times the mean standard deviation across all channels.

The preprocessed EEG data were then divided into epochs of 3.5 s (total duration), including 1 s pre-cue interval, 500 ms cue presentation, 1 s cue-stimulus interval and 1 s post-stimulus interval. Epochs having a joint probability of activity greater than three standard deviations were automatically rejected. If for one experiment more than 30% of epochs were rejected, the data for that participant were excluded from further analysis.

Subsequently, electrophysiological data were analysed using the FieldTrip toolbox (http://fieldtriptoolbox.org) [35] for Matlab (Mathworks, Inc. USA).

Two analyses were performed on epoched data (i) by performing a time-frequency decomposition, and (ii) by calculating the VEPs. VEPs were generated by averaging at the individual level the activity across trials and applying a baseline correction (-100 to 0ms). To avoid biasing classification results, the VEPs of each participant in each experiment were normalized [36].

Time-frequency analyses were conducted per channel using a wavelet transform, known to represent a compromise between time and frequency resolution [37]: the procedure is fully described in the SI (section 3.3). The wavelet transform was conducted on an interval from -1 to 2.5 sec after stimulus onset, in time steps of 20 ms. The data transformation was performed before averaging across trials, separately for each frequency band. The total power of each frequency band represents both the phase-locked and the non-phase-locked signal with respect to the event. The resulting power was baseline corrected to obtain the relative signal change ($Pcorr$) which constituted the input of subsequent group-analyses. The pre-stimulus period between -300 to -200 ms was used as a baseline for all spectral analyses. This baseline avoids inclusions of slow frequency leakage occurring immediately before the stimulus onset (please refer to section 3.4 of the SI for further information).

ACCEPTED MANUSCRIPT

Downloaded from https://academic.oup.com/pnasnexus/advance-article/doi/10.1093/pnasnexus/pgaf288/8249480 by guest on 16 September 2025

Statistical analyses

Each of the data analyses described below was repeated for Experiment 1 and 2. Analyses were focused on exploring VEPs and time-frequency modulation as a function of the different evaluation tasks (aesthetic *vs.* pragmatic).

Statistical analyses in the time-frequency domain. Oscillatory fingerprints [38] of aesthetic vs. pragmatic evaluations were separately assessed for the (i) pre- and (ii) post-stimulus onset period with the same statistical approach. To investigate the possible effects of the evaluation task (aesthetic *vs.* pragmatic) separately on pre (from -1s to 0) and post-stimulus (from 0 to 1s) oscillations, we employed a cluster-based permutation approach that accounts for the multiple comparison problem [39]. The effect at the sample level was quantified by means of two-tailed t-tests for dependent samples comparing the time-frequency oscillation between conditions (aesthetic and pragmatic) in a wide spectrum (2-40 Hz) and at each time point and channel (n=62). Further details on the statistical approach (i.e., the two-tailed t-test corrected by cluster-based permutations) are included in the SI (section 3.5). We hypothesized that aesthetic and pragmatic evaluations affected alpha oscillations in both the pre-stimulus onset period and the post-stimulus onset period.

Statistical analyses in the time domain. To investigate the effects of the evaluation task (aesthetic vs. pragmatic) on the magnitude in time of the brain response, first, we extracted two average waveforms (VEPs) for each participant, one corresponding to the aesthetic judgements and the other to the symmetry ones. Group-level statistics and correction for multiple comparisons were performed via cluster-based permutation testing [39], analogously to the time-frequency analyses described above. Specifically, differences between conditions (aesthetic vs. symmetric) in the time domain were quantified by means of two-tailed t-tests for dependent samples. We compared the baseline corrected evoked response between tasks (aesthetic and pragmatic) at all latencies (from 0 to 2.5s) and channels (n=62). Clusters were identified based on temporal and spatial proximity, and the algorithm selected the t-values exceeding a specified threshold (cluster alpha= 0.05), as explained above in the previous section and the SI (section 3.6).

ACCEPTED MANUSCRIPT

Downloaded from https://academic.oup.com/pnasnexus/advance-article/doi/10.1093/pnasnexus/pgaf288/8249480 by guest on 16 September 2025

Machine learning approach

In the binary classification problem, our goal was to employ the features of alpha power measured pre and post stimulus onset (pre-stimulus inhibitory alpha power and post-stimulus alpha ERD) and the VEP recorded in the first 200 ms post stimulus onset (including the C1 and the N170) to predict the pragmatic vs. aesthetic nature of the task. The classification was performed first within Experiment 1 and then using the data of Experiment 1 as the training set and the data of Experiment 2 as the test set. The precise mathematical model that we used in the machine learning analysis is fully described in the SI (section 4).

Results

All participants (N=36) recruited in the study were included in the group level analysis. As descriptive analyses of the images employed, we investigated the aesthetic judgements provided during the aesthetic task. The statistical comparison between the average aesthetic appreciation of synthetic (mean = 4.53; s.d. = 1.155) and natural (mean = 5.47; s.d. = 0.900) images revealed that they differed significantly. More specifically, natural images showed significantly higher appreciation than synthetic ones (paired-sample t-test results: mean = -1.10; s.d. = 0.179; t_{35} = -6.16; $p < 0.001$; Cohen's dz = 1). With the aim of exploring possible determinants of participants' aesthetic judgements beside other low-level statistical features (such as contrast and luminosity, which were counterbalanced across blocks and conditions - see Methods and Stimuli), through Mid-level Vision ToolBox [22], we quantified the curvature value of each image, since image curvature has often been associated with image beauty [40]. In the present study too, we found a significant relation between natural (but not synthetic) images and curvilinearity in the aesthetic task (for further details on these descriptive analyses, please refer to the SI).

ACCEPTED MANUSCRIPT

Downloaded from https://academic.oup.com/pnasnexus/advance-article/doi/10.1093/pnasnexus/pgaf288/8249480 by guest on 16 September 2025

Testing Hypothesis 1: Results in the time-frequency domain

The time-frequency transformation of the neural signal obtained in both tasks (aesthetic and pragmatic) within each experiment revealed the expected frequency-power spectrograms as a function of time, expressed through a logarithmic distribution. Figures 4A and 4D show the differences in average power spectrum between the aesthetic and the pragmatic task, respectively in Experiment 1 and 2, in the pre-stimulus comparison (i). Figures 4B and 4E instead present the spectrograms of the same contrast (aesthetic vs pragmatic task in both Experiment 1 and 2) estimating the percent change in post-stimulus neural oscillation (ER%) relative to the baseline (−0.3 to −0.2 s before stimulus onset). ER% changes constituted the input for subsequent post-stimulus analyses (ii).

Experiment 1 (synthetic images). (i) The cluster-based statistical comparison of the pre-stimulus power spectrum (from -1 to 0 s) displayed a significant decrease in alpha and beta frequency power in the aesthetic task compared to the pragmatic task (cluster $p = 0.03$; Figure 4C). More specifically, this analysis (aesthetic vs pragmatic task) revealed a significant negative cluster indicating a significant decrease of alpha power (between 8 and 11 Hz), in a time window between -0.7 and -0.5 s over a cluster of centro-parietal channels (P3, Pz, P1, p2, CP3, CP1, CPz, C1, FC5, P4). Additionally, the statistical comparison revealed a significant decrease of beta power (between 18 and 35 Hz) in two different time windows: the first between -0.8 and -0.6 s and the second between -0.5 and -0.3 s, over a cluster of centro-occipital channel (P3, P7, CP1, CP5, P1, CP3, P5, O1, PO3, PO7, FC5, C5, C1, TP9, Oz).

However, when restricting the statistical comparison to the alpha frequency band (8-12 Hz) only, the resulting negative cluster did not reach statistical significance ($p = 0.065$).

(ii) The cluster-based comparison of the post-stimulus power spectrum (from 0 to 1 s) between aesthetic and pragmatic evaluation tasks revealed no significant difference (negative cluster, $p = 0.11$). The statistical comparison on the alpha frequency band only (8-12 Hz) did not reveal any significant cluster (negative cluster, $p = 0.3$).

ACCEPTED MANUSCRIPT

Downloaded from https://academic.oup.com/pnasnexus/advance-article/doi/10.1093/pnasnexus/pgaf288/8249480 by guest on 16 September 2025

Experiment 2 (natural images). (i) The statistical comparison of the pre-stimulus power spectrum (from -1 to 0 s) displayed a significant decrease in alpha and beta power in the aesthetic vs pragmatic task (cluster p = 0.04; Figure 4F). The analysis (aesthetic vs pragmatic) revealed a significant decrease of alpha power (between 10 and 12 Hz), in a time window between -0.8 and -0.2 s, within a large cluster of centro-parietal channels (O1, O2, Iz, Oz, PO4, P4, P2, CP3, C3, C5, FC5, F5, TP9, P7, PO5, P5). Furthermore, the same comparison (aesthetic vs pragmatic) also revealed a significant decrease of beta power (between 25 and 35 Hz), in a time window comprised between -0.8 and -0.4 s over a cluster of parieto-occipital channels (P3, P4, Pz, P1, p2, PO3, PO4, POz, Oz, O2, C3, Cz, C1, P5, CP1, CP3, CP2).

The statistical comparison restricted to the alpha frequency band (8-12 Hz) revealed a significant negative cluster (p = 0.03) involving parieto-occipital channels (C3, P3, P4, O1, O2, F7, T7, P7, Pz, Iz, FC1, CP1, CP2, FC5, CP5, TP9, P1, P2, CP4, PO3, PO4, F5, C5, P5, AF7, FT7, TP7, PO7, PO8, CPz, POz, Oz) in a time window between -0.68 and -0.3.

(ii) The comparison of the post-stimulus power spectrum (from 0 to 1 s) between aesthetic and pragmatic evaluation tasks did not reveal any significant cluster (positive cluster, p = 0.21). The comparison restricted to the alpha frequency band (8-12 Hz) also revealed no significant difference (positive cluster, p = 0.06).

Testing Hypothesis 1: Results in the time domain (VEPs)

The grand average waveforms elicited during the evaluation tasks in both experiments are shown in Figure 3 and reveal a typical VEP response associated with visual stimulus processing [9] and evaluation [14,15]. We observed the expected early components within the first 200 ms, namely the C1 and N170 components [10], followed by a slow rising positivity, emerging around 0.3 s, and most likely corresponding to the Late Positive Potential (LPP), a component often associated with evaluation tasks [14,15].

Experiment 1 (synthetic images). Point-by-point, group-level analyses over the time window 0 - 1 s revealed a significant positive cluster (p = 0.045) extending from 0.472 to 0.712 s post-

Downloaded from https://academic.oup.com/pnasnexus/advance-article/doi/10.1093/pnasnexus/pgaf288/8249480 by guest on 16 September 2025

ACCEPTED MANUSCRIPT

stimulus onset, indicating more positive neural response during the aesthetic vs pragmatic task. This cluster was distributed across a broad group of fronto-parietal channels (F3, C3, F7, T7, T8, P7, Iz, FC5, TP9, TP10, AF3, FC3, PO3, F5, C5, AF7, FT7, TP7, TP8, PO7, PO8, O1, Oz).

The cluster-based statistic limited to the first 0.2 s (0 - 0.2 s) did not reveal any significant differences (negative cluster, p = 0.2). Similarly, when directly comparing the peak amplitudes of the C1 and N170 components across the two evaluation conditions, no significant cluster was found.

Experiment 2 (natural images). Point-by-point, group-level analyses over the post-stimulus time window (0 – 1 s) revealed two different clusters of significance (aesthetic vs pragmatic). The first cluster of significance (i.e., positive cluster, p = 0.03) encompassed a broad scalp distribution (FP2, F3, F4, P4, 01, 02, T7, T8, P7, P8, Fz, Iz, FC2, CP2, FC5, FC6, CP5, CP6, TP9, TP10, P2, AF3, FC3, FC4, CP3, CP4, PO3, PO4, C6, P5, P6, TP7, TP8, PO7, PO8, Oz) in a time window interval between 0.380 and 0.500 s. The second positive cluster (p = 0.006) involved a large number of fronto-central channels (F3, C3, C4, P3, P4, 01, 02, T7, T8, P7, P8, Fz, Iz, FC2, CP2, FC5, FC6, CP5, CP6, TP9, TP10, P2, AF3, FC3, FC4, CP3, CP4, PO3, PO4, C6, P5, P6, TP7, TP8, PO7, PO8, Oz) in a time window between 0.596 and 0.980 s.

The cluster-based statistic restricted to the 0 - 0.2 s interval did not reveal any significant differences (negative cluster, p = 0.2). When directly comparing the peak amplitudes of the C1 and N170 components across the two evaluation conditions, the point-by-point statistics revealed two significant clusters, within the time window centred on the peak of the N170 component (0.128 - 0.168 s). The first positive cluster (p = 0.01) involved a number of fronto-parietal channels (Fp1, Fp2, F3, F7, T7, FC5, CP5, TP9, F1, AF3, F5, C5, AF7, FT7, TP7, Fpz) in the time window between 0.128 and 0.164 s, while the second positive cluster (p = 0.03) involved a cluster of parieto-occipital channel (O1, O2, P8, Iz, TP10, F6, C6, TP8, PO8, Oz) in the same time window.

To sum up, with Hypothesis 1 we expected to observe in both experiments decreased pre-stimulus inhibitory alpha power and increased post-stimulus alpha ERD and VEP early

ACCEPTED MANUSCRIPT

Downloaded from https://academic.oup.com/pnasnexus/advance-article/doi/10.1093/pnasnexus/pgaf288/8249480 by guest on 16 September 2025

components in the aesthetic task compared to the pragmatic one. Results on the pre-stimulus activity fully confirmed our hypothesis, both for Experiment 1 and 2, demonstrating the presence of a different preparatory activity across tasks. However, we did not find any difference in the neural oscillatory activity of the post-stimulus. Results on VEPs (0-1 s time window) revealed a significant difference across the two tasks encompassing the LPP time window. Significant differences within VEP early components were found for Experiment 2 selectively, within the N170 time window.

Testing Hypothesis 2: Machine learning approach

To assess whether the aesthetic and pragmatic tasks could be predicted within conditions and across experiments by the neural activity, we implemented four different analytical approaches that exploited in different manners information contained across participants, features and electrodes, and using two different classifiers (linear binary classifier and SVM).

(1) First, as described in the supplementary material we employed a linear binary classifier across participants (using a half-split approach) and across features, to investigate the possibility of distinguishing between pragmatic and aesthetic judgments separately for each experimental condition (i.e., synthetic and natural images), as well as across conditions through cross-decoding (i.e., training on synthetic images and testing on natural ones).

More specifically, features were employed in a multivariate classifier, neglecting the spatial informativeness of the channels. Given the visual nature of the task, we averaged the activity of evoked and oscillatory neural responses across two posterior channels (O1 and O2), which well capture visual responses for both ERPs and time-frequency data. For the whole set of the aforementioned features (i.e., C1, N170, alpha pre-stimulus, and alpha post-stimulus, which were the average of the activity within the relative time windows), we trained and tested a linear binary classifier across participants (half the subjects as training and half as test), based on the data associated with synthetic images coming from Experiment 1, using the procedure described in the supplementary material, hence including $|H| = 161051$ candidate classifiers in the optimization process. For completeness, we repeated the procedure using data associated

ACCEPTED MANUSCRIPT

Downloaded from https://academic.oup.com/pnasnexus/advance-article/doi/10.1093/pnasnexus/pgaf288/8249480 by guest on 16 September 2025

with natural images coming from Experiment 2. Then, based on the same procedure, we trained a linear binary classifier using data associated with synthetic images coming from Experiment 1 for the training set (including data from all subjects in that set), and data associated with natural images coming from Experiment 2 as test set (including data from all subjects in that set). For each analysis, to assess the performance of the best classifier on the test set, we applied again Hoeffding's bound, this time with the empirical risk evaluated on the test set, and with the Statistical Learning Theory (SLT)-based confidence half-interval ε evaluated using $|H| = 1$, since only one classifier had to be tested. Finally, for the first two analyses, the procedure was repeated, exchanging the training and test sets. In this way, it was possible to estimate the (best-classifier) classification error rate per subject. For the third (cross-experimental) analysis, this exchange was not needed, being it was already possible to estimate the (best-classifier) classification error rate per subject. Significance was tested against chance level (i.e., 50%) using a one-sample, one-tailed t-test (n = 36, right-tailed).

ML Results. (1) Starting from the raw data, feature vector normalization was obtained by dividing each feature vector by its l1-norm (i.e., the sum of the absolute values of its components). For Experiment 1, the size of the training set turned out to be slightly smaller than 3136, since some low-quality acquisitions (among the 180 trials obtained per subject) were not included in the dataset. As a consequence, the SLT-based confidence half-interval ε in Hoeffding's bound was recalculated, taking into account the actual training set size, turning out to be slightly larger than 0.05 or 5% (which is the value reported in the supplementary material). In the application of Hoeffding's bound, the confidence parameter was chosen as $\eta = 0.05$. The results are summarized as follows:

a) For Experiment 1, the minimum classification error rate on the training set was 47.4%, with an SLT-based confidence half-interval ε equal to 5.3%. Hence, based on data coming from the training set, Hoeffding's bound on the classification error rate of the best classifier turned out to be 52.7%. The classification error rate of the best classifier on the test set was 50.6%, whereas the associated SLT-based confidence half-interval ε was 2.6%. Hence, based on data coming from the test set, Hoeffding's bound on the classification error rate of the best classifier

ACCEPTED MANUSCRIPT

Downloaded from https://academic.oup.com/pnasnexus/advance-article/doi/10.1093/pnasnexus/pgaf288/8249480 by guest on 16 September 2025

turned out to be 53.2%. Test-set classification error rates extracted for each participant and tested against 50% revealed that the classification was not different from chance level.

b) For Experiment 2, the minimum classification error rate on the training set was 47.5%, with an SLT-based confidence half-interval ε equal to 5.3%. Hence, based on data coming from the training set, Hoeffding's bound on the classification error rate of the best classifier turned out to be 52.8%. The classification error rate of the best classifier on the test set was 47.6%, whereas the associated SLT-based confidence half-interval ε was 2.6%. Hence, based on data coming from the test set, Hoeffding's bound on the classification error rate of the best classifier turned out to be 50.2%. As for Experiment 1 test-set classification error rates extracted in each participant tested against 50% revealed that the classification was not different from chance level and test-set classification error rates per subjects and tested against 50% revealed that the classification was not different from chance level.

c) For the cross-experimental analysis, the minimum classification error rate on the training set was 48.3%, with an SLT-based confidence half-interval ε equal to 3.7%. Hence, based on data coming from the training set, Hoeffding's bound on the classification error rate of the best classifier turned out to be 52.0%. The classification error rate of the best classifier on the test set was 49.0%, whereas the associated SLT-based confidence half-interval ε was 1.8%. Hence, based on data coming from the test set, Hoeffding's bound on the classification error rate of the best classifier turned out to be 50.8% and test-set classification error rates per subjects tested against 50% revealed that the classification was not different from chance level.

In sum, results of the first ML approach did not allow to classify pragmatic and aesthetic judgments once for Experiment 1, 2 and across experiments.

Exploratory ML analysis. We further assessed whether the machine learning approach would allow distinguishing the two tasks (aesthetic and pragmatic) by running three additional tests, starting from the use of all available information, and decrementally exploiting less information contained in the datasets. This allowed to infer the relative importance of each data dimension.

(2) We run a Support Vector Machine (SVM) classifier to assess, within each experimental condition (i.e., synthetic and natural images) and separately for each feature of interest, the

ACCEPTED MANUSCRIPT

Downloaded from https://academic.oup.com/pnasnexus/advance-article/doi/10.1093/pnasnexus/pgaf288/8249480 by guest on 16 September 2025

capacity to distinguish between pragmatic and aesthetic judgments, across electrodes and participants, and conditions through cross-decoding (i.e., training on synthetic images and testing on natural ones). Specifically, for each of the aforementioned features (i.e., C1, N170, alpha pre-stimulus, and alpha post-stimulus), we trained and tested an SVM classifier across all EEG channels, separately for synthetic and natural images, participants, and folds (for the cross-validation).

(3) The same approach as in (2) was run at the single participant level but across features. Specifically, we used all features in a multivariate model (i.e., C1, N170, alpha pre-stimulus, and alpha post-stimulus; note in the previous approach ML was performed for each feature independently) and we trained and tested an SVM classifier across all EEG channels, separately for synthetic and natural images, participants, and folds.

(4) Finally, we run a Support Vector Machine (SVM) classifier using a half-split approach (analogously to the first method reported in *Testing Hypothesis 2: Machine learning approach*) and across features after averaging the activity of evoked and oscillatory neural responses across two posterior channels (O1 and O2).

For approaches using single participant data (2 and 3), we employed a 10-fold cross-validation (with stratified sampling; linear kernel; C hyperparameter - BoxConstraint - optimized during training via a 50-step grid search). For the cross-decoding procedure (again of 2 and 3), in each participant, we trained the SVM classifier using all the synthetic images and tested on the natural ones (linear kernel; C hyperparameter optimized via a 50-step grid search). Data from 62 EEG channels were normalized (z-scoring each channel using mean and standard deviation estimated only in the training set the data) independently for channel each using mean and standard deviation estimated only in the training set, trial and used as predictors, while the target variable was a binary vector encoding pragmatic and aesthetic judgments across trials. Accuracy and F1-score (i.e., the harmonic mean of precision and recall for the aesthetic class) were calculated for each participant and condition. Average accuracy, F1-score, and their standard errors were estimated across all the participants. Significance was tested against chance level (i.e., 50%) using a one-sample, one-tailed t-test (n = 36, right-tailed). P-values were

ACCEPTED MANUSCRIPT

Downloaded from https://academic.oup.com/pnasnexus/advance-article/doi/10.1093/pnasnexus/pgaf288/8249480 by guest on 16 September 2025

corrected for multiple comparisons across features and experimental conditions using the Bonferroni method.

Overall, the different ML approaches (1-4) allowed to infer the role of the shared informativeness of the type of image (with cross experiment decoding), participants (with half split or single subject analyses), features (testing them in isolation or as a multivariate input), and electrodes (all of them or only posterior).

ML Results of the exploratory analysis. (2) Results for the ML approach exploiting all informativeness of the dataset (single subjects, single feature, across all electrodes) showed that for both synthetic and natural images, post-stimulus evoked and pre-stimulus oscillatory neural activity allowed disentangling between pragmatic and aesthetic judgments (see Figure 5). In particular, accuracy for synthetic images was significantly different from chance for feature N170 (mean Accuracy ± Standard Error = 55.7 ± 1.4 %, p_{Bonf} = 0.002, F_1-score = 54.5 ± 1.9 %), and for pre-stimulus alpha activity (Accuracy r = 61.1 ± 1.8 %, p_{Bonf} = 0.000001, F_1-score = 61.3 ± 1.9 %). Accuracy for natural images was significantly different from chance for N170 (Accuracy = 55.0 ± 1.0 %, p_{Bonf} = 0.0001, F_1-score = 51.8 ± 2.3 %), and for pre-stimulus alpha activity (Accuracy = 59.4 ± 1.5 %, p_{Bonf} = 0.000003, F_1-score = 60.0 ± 1.6 %). For both synthetic and natural images the feature C1 and alpha post-stimulus were not providing significant results. Conversely, cross-decoding (i.e., training on synthetic images and testing on natural ones, independently for each participant) was not successful for any of the features.

(3) Results showed that for both synthetic and natural images, the four features combined allowed disentangling between pragmatic and aesthetic judgments. In particular, accuracy for both synthetic and natural images was significantly different from chance (mean Accuracy ± Standard Error = 54.4 ± 1.2 %, p_{Bonf} = 0.002, F1-score = 49.9 ± 3.6 %; Accuracy = 53.3 ± 0.8 %, p_{Bonf} = 0.0005, F1-score = 43.6 ± 3.6 %). As for the previous analytical approach, cross-decoding (i.e., training on synthetic images and testing on natural ones across features and independently for each participant) was not successful.

(4) Results showed that with this approach, only for natural images the four features combined allowed disentangling between pragmatic and aesthetic judgments (mean Accuracy ± Standard

ACCEPTED MANUSCRIPT
Downloaded from https://academic.oup.com/pnasnexus/advance-article/doi/10.1093/pnasnexus/pgaf288/8249480 by guest on 16 September 2025

Error = 52.1 ± 0.8 %, p_{Bonf} = 0.03, F1-score = 53.7 ± 1.4 %). As for all analytical approaches, cross-decoding (i.e., training on synthetic images and testing on natural ones across features and independently for each participant) was not successful.

Discussion

The present study aimed to explore, with solid a priori assumptions and a fully pre-registered design, the age-old intuition that aesthetic experiences are characterised by a state of heightened attention towards external stimuli (i.e., an "aesthetic attitude"). Specifically, we examined whether engaging in sustained aesthetic evaluation, as opposed to pragmatic one, recruits distinct neural processes and generates a top-down, tonic attentional enhancement observable by measuring pre-stimulus and post-stimulus attention-related indexes in the EEG signal. Overall, our findings both in the time and time-frequency domains support this hypothesis, revealing different evoked response and oscillatory activity across tasks, even though not all our predictions were confirmed (see § Results, "Testing Hypothesis 1"). The machine learning approaches, solved the binary classification problem only when run at the single participant level, showing that the N170 component and alpha oscillatory activity before stimulus onset can predict the assigned task within the same experiment, but not across different experiments (see § Results - Testing Hypothesis 2), suggesting highly consistent effects across trials, within the same experiment.

Neural oscillatory dynamics during aesthetic evaluation

The pre-stimulus time-frequency results of both experiments (synthetic and natural images) revealed a significant tonic decrease in alpha (8 - 12 Hz) and beta (20 - 30 Hz) frequency power during aesthetic compared to pragmatic evaluation, fully supporting our first hypothesis. This result points out that participants' oscillatory activity differs significantly even before the onset of the image, suggesting the emergence of a specific "attitude" during the evaluation task, in full support of our first hypothesis. Importantly, pre-stimulus alpha power reduction has been

ACCEPTED MANUSCRIPT

Downloaded from https://academic.oup.com/pnasnexus/advance-article/doi/10.1093/pnasnexus/pgaf288/8249480 by guest on 16 September 2025

associated in the literature with attentional engagement [41] and perceptual processing facilitation (enhanced gain of the visual stream [41]). It is therefore possible that one of the processes characterizing aesthetic evaluation is an enhanced allocation of neural resources toward the processing of attended stimuli. Moreover, the observed pre-stimulus tonic reduction in alpha and beta power has frequently been reported during preparatory activity and is typically associated with the so-called *Readiness potential* (RP) [42–44] . The RP, traditionally linked to motor preparation [42], has more recently been observed in cognitive tasks as well [42–45], such as preparing for mental operations on numbers [43]. Therefore, in line with previous studies investigating the preparatory activity indexed by RP [42,44,46] in motor and cognitive tasks, it is possible that the reduction in beta power during the aesthetic task reflects an enhanced preparatory process, while the accompanying decrease in alpha power may be interpreted as the complementary attentional engagement, both promoting a sensory-oriented engagement with the upcoming stimuli. To sum up, our results on the pre-stimulus interval reveal a distinct neural signature, likely reflecting attentional and preparatory processes, linked with the aesthetic task.

On the other hand, the post-stimulus time-frequency analysis of Experiments 1 and 2 did not support our a priori hypothesis. We observed no significant difference in alpha ERD between the aesthetic and pragmatic evaluation tasks. This suggests that the oscillatory activity following stimulus onset was not modulated by the specific evaluation task. However, when considered alongside the significant differences observed in VEP responses (see below), our findings indicate that post-stimulus neural activity differs markedly in terms of amplitude and latency across tasks, even though not in the frequency band hypothesized. Several factors may account for the discrepancies observed between time domain and time-frequency responses. One possibility is that the significant pre-stimulus difference in the alpha and beta bands affected post-stimulus analyses, potentially limiting the detection of significant ER% effects. Future studies could be directed to disentangle pre- and post- stimulus time-frequency dynamics by designing both the experimental protocol and the statistical approach to address this issue more effectively.

Downloaded from https://academic.oup.com/pnasnexus/advance-article/doi/10.1093/pnasnexus/pgaf288/8249480 by guest on 16 September 2025

ACCEPTED MANUSCRIPT

VEP responses modulation between aesthetic and pragmatic tasks

The time domain results partially confirmed our first hypothesis, revealing significant differentiation of the VEPs between aesthetic and pragmatic tasks (see § Results and Figure 3). Aesthetic *vs* pragmatic evaluation of synthetic images (Experiment 1) elicited a significant modulation of the LPP, predominantly over the left hemisphere. However, the earlier time window (0-200 ms) did not reveal a significant difference between tasks, suggesting that the aesthetic evaluation did not modulate the C1 and N170 early components in synthetic images. On the other hand, VEPs elicited by natural images (Experiment 2) revealed three clusters of significant difference, encompassing a larger and distributed scalp topography, and involving both the LPP (from its onset) and the N 170 component. The findings from Experiment 2 support our first hypothesis, suggesting that during the aesthetic evaluation of natural images, participants engaged in distinct neural processes as early as 200 ms post-stimulus. To sum up, aesthetic evaluation consistently enhanced the LPP across both experiments, confirming previous findings and extending them by revealing an earlier onset and a broader scalp distribution [14,15]. The LPP is a well-established ERP component emerging between 300 and 1200 ms after stimulus onset and is associated with sustained attentional and evaluative processes, especially in response to emotionally salient stimuli [47]. Notably, both the latency and scalp distribution of the LPP provide valuable information for distinguishing its functionally distinct temporal components [48]. The early LPP (300 – 600 ms), typically associated with a posterior topography, is thought to reflect automatic attentional engagement and emotional reactivity [48–51]; the late LPP (600 – 1200 ms), characterized by a broader anterior-posterior distribution, is generally connected with prefrontal cortical involvement and is associated with cognitive regulation and deliberative evaluation [48,52]. Crucially, task instructions, such as providing information about stimulus valence, have been shown to differentially modulate these LPP components, affecting both appraisal and reappraisal processes [48,53,54]. Our findings revealed an earlier onset of LPP differentiation compared to prior studies on aesthetic appreciation processes [14,16,18], indicating that our design might have induced modulation of both the early and late LPP components. Moreover, while Jacobsen and colleagues reported a predominantly right-hemisphere distribution, our results showed a left-lateralized topography in Experiment 1

ACCEPTED MANUSCRIPT

Downloaded from https://academic.oup.com/pnasnexus/advance-article/doi/10.1093/pnasnexus/pgaf288/8249480 by guest on 16 September 2025

and a broader, more distributed activation in Experiment 2 [14]. We speculate that our paradigm, specifically designed to induce sustained aesthetic evaluation over time, successfully elicited a stronger aesthetic attitude, persisting throughout the entire experimental block. This enduring state likely modulated both early and late LPP components and thus influenced both affective and higher-order cognitive evaluative processes.

As indicated in the Results, image type (synthetic *vs* natural) influences the VEP responses during aesthetic and pragmatic evaluation, showing distinct temporal and spatial clusters of significance across experiments. Specifically, the sustained aesthetic evaluation of natural images when compared to synthetic images elicited a broader (i.e., bilateral) and earlier differentiation, also involving the N170 component. This finding suggests that the aesthetic attitude effect was amplified by natural images. One contributing factor may be the generally higher aesthetic appreciation of these stimuli compared to synthetic ones (see Results). Participants' clear preference for natural scenes may have fostered the engagement with the aesthetic evaluation task. Additionally, the semantic richness typically associated with landscapes (and fully absent in synthetic images) may have further enhanced the effect observed in Experiment 2. Future studies should investigate the influence of aesthetic appreciation on the establishment of a strong aesthetic attitude, ideally by controlling for both stimulus low-level features and subjective preferences.

Neural signatures differentiate between aesthetic and pragmatic tasks

The machine learning approach successfully addressed the binary classification problem, but only partially fulfilled the two a priori predictions. Specifically, the N170 component and pre-stimulus alpha oscillatory activity were able to predict the assigned task within the experiment, but failed to generalize across experiments (see Figure 5). Note that this finding emerged only once the analysis was performed at the single participant level, suggesting variability across individuals of the effects.

This finding reinforces previous discussions, suggesting that neural signatures in both pre-stimulus and early post-stimulus windows (within 200 ms) are reliable task predictors. Notably,

Downloaded from https://academic.oup.com/pnasnexus/advance-article/doi/10.1093/pnasnexus/pgaf288/8249480 by guest on 16 September 2025

ACCEPTED MANUSCRIPT

the ML also identified a role for the N170 in the synthetic experiment, an effect not detected by the VEP cluster-based statistical analysis, thereby highlighting the enhanced sensitivity of the ML approach. The lack of predictive accuracy across experiments provides empirical confirmation of previously observed differences in the neural signals between Experiments 1 and 2 and thus between the neural activity associated with the use of synthetic and natural stimuli. Variations in pre-stimulus oscillatory activity, VEP latency and amplitude, as well as differences in scalp distribution, make it impossible to generate predictions across tasks. Nevertheless, the ML approach provided further evidence of the possibility to use biomarkers to differentiate between aesthetic experiences from other forms of visual judgments.

The neural underpinnings of the aesthetic attitude

Overall, our results shed some light on the age-old philosophical idea that our experiences of beauty are characterised by the adoption of a special mode of attention - heightened, contemplative and focused on the object's formal or expressive qualities (i.e., the "aesthetic attitude") [1,2,13]. This idea, central to classical aesthetics especially in the Kantian tradition, is increasingly gaining traction in psychology and neuroscience, where evidence for a distinctive attentional state in aesthetic contexts is beginning to accumulate. Previous neuroscientific findings have suggested that a state of heightened attention during engagement with art may be supported by alpha-band oscillation [55,56]. Distinctive neural responses in aesthetic contexts appear to be generable through top-down processes, such as engaging in aesthetic evaluation [15,16,18] or being exposed to aesthetically appealing stimuli that generate expectations of encountering other appealing stimuli [55–57]. However, many aspects of the relationship between aesthetic experiences and attention remain unclear. In particular, it is unclear whether tasks of aesthetic evaluation can systematically induce observable attentional enhancements.

Our results contribute to filling this gap by offering a rigorous, data-driven exploration of how an aesthetic evaluation task can produce a top-down modulation of well-established EEG indexes of perceptual and attentional enhancement. The systematic modulation of neural oscillatory activity in both alpha and beta frequency bands prior to stimulus presentation, the predictive role of early VEP components in distinguishing the task (aesthetic vs pragmatic), and

ACCEPTED MANUSCRIPT

Downloaded from https://academic.oup.com/pnasnexus/advance-article/doi/10.1093/pnasnexus/pgaf288/8249480 by guest on 16 September 2025

the observed enhancement of both the early and late components of the LPP, all support the idea that participants were adopting a distinctive processing mode when evaluating images for their aesthetic appeal. This extends previous findings on the neural correlates of evaluative tasks [14–16,18] and shed some new light on the neural underpinnings of the aesthetic attitude.

In this respect, our study may represent the experimental evidence of a growing body of research linking aesthetic experience to enhanced perceptual processing and attentional magnification. According to several recent theoretical frameworks, we experience aesthetic pleasure when we are particularly effective in processing sensory information (i.e., we process information fluently, we find new patterns in our sensorium, we make larger updates to our models of the world, we experience faster reduction in uncertainty about the causes of our sensations) [7,58–60]. Aesthetic pleasure acts as a kind of hedonic feedback that signals which portions of the world are more informatively profitable and worth exploring further [7]. Interestingly for our purposes, according to several of these approaches, aesthetic pleasure does not merely act as a feedback of effective perceptual processing, but can also generate the expectation that future perceptual encounters will be specially profitable, making us more attentive, curious, and inclined to learn. Previous studies have shown that exposure to aesthetically pleasing stimuli enhance attention, perceptual learning processing and curiosity in subsequent tasks. [55,57,61,62]. Our study extends this result by showing that the mere framing of a task in terms of aesthetic appreciation can lead to appreciable perceptual and attentional enhancements. In particular, our findings suggest that an aesthetic attitude can be induced by a purely top-down instruction, and then be sustained and increased by the pleasantness of the stimuli presented, in a sort of non-linear but exponential process. We speculate that this may be particularly relevant in the context of profound aesthetic experiences, such as those elicited by museum visits, music, cinema and theatre, where both the expectation to encounter beauty and the sustained encounter with beautiful stimuli contribute significantly to the overall experience.

This study has the potential to inform different fields that could benefit from a better understanding of the way in which we deploy our attentional resources, such as education,

ACCEPTED MANUSCRIPT

Downloaded from https://academic.oup.com/pnasnexus/advance-article/doi/10.1093/pnasnexus/pgaf288/8249480 by guest on 16 September 2025

psychotherapy [63], neurocognitive rehabilitation [64] and social adaptation in times of distress [65]. Adopting an aesthetic perspective may prepare the neural system to embrace the sensory, cognitive, and affective complexity of the environment, effectively tuning the perceiver to its informativeness.

Acknowledgements

IR was funded by PON project "Ricerca e Innovazione" 2014-2020 (Italian Ministry of University and Research; D11B21005800007); FP and JF are funded by PNRR project NODES (European Union – Next Generation EU: D17G22000150001; Italian Ministry of University and Research). DB was funded by PRIN 2017 (20177894ZH). This project is also funded by a Micro Grant awarded to JF by the Division 10 of the American Psychological Association. The funders have/had no role in study design, data collection and analysis, decision to publish or preparation of the manuscript.

References

1. Stolnitz, J. ' The Aesthetic Attitude' in the Rise of Modern Aesthetics. *J. Aesthet. Art Crit.* **36**, 409–422 (1978).
2. Kant, I. *Critique of the Power of Judgment*. (Cambridge University Press, 2000).
3. Perlovsky, L. I. Neural mechanisms of the mind, Aristotle, Zadeh, and fMRI. *IEEE Trans. Neural Netw.* **21**, 718–733 (2010).
4. Bullough, E. Psychical distance as a factor in art and an aesthetic principle. *Br. J. Psychol.* **5**, 87 (1912).

Downloaded from https://academic.oup.com/pnasnexus/advance-article/doi/10.1093/pnasnexus/pgaf288/8249480 by guest on 16 September 2025

ACCEPTED MANUSCRIPT

5. Weigand, R. & Jacobsen, T. Interruption, work rumination, and stress as indicators of reduced working memory resources affect aesthetic experiences. *Q. J. Exp. Psychol.* **75**, 1272–1288 (2022).
6. Weigand, R. & Jacobsen, T. Beauty and the busy mind: Occupied working memory resources impair aesthetic experiences in everyday life. *PloS One* **16**, e0248529 (2021).
7. Sarasso, P., Neppi-Modona, M., Sacco, K. & Ronga, I. “Stopping for knowledge”: The sense of beauty in the perception-action cycle. *Neurosci. Biobehav. Rev.* **118**, 723–738 (2020).
8. Vartanian, O. & Goel, V. Neuroanatomical correlates of aesthetic preference for paintings. *Neuroreport* **15**, 893–897 (2004).
9. Nadal, M. The experience of art: Insights from neuroimaging. *Prog. Brain Res.* **204**, 135–158 (2013).
10. Sarasso, P. *et al.* Beauty in mind: Aesthetic appreciation correlates with perceptual facilitation and attentional amplification. *Neuropsychologia* **136**, 107282 (2020).
11. Klimesch, W. Alpha-band oscillations, attention, and controlled access to stored information. *Trends Cogn. Sci.* **16**, 606–617 (2012).
12. Pfurtscheller, G., Neuper, C. & Mohl, W. Event-related desynchronization (ERD) during visual processing. *Int. J. Psychophysiol.* **16**, 147–153 (1994).
13. Pelowski, M., Markey, P. S., Forster, M., Gerger, G. & Leder, H. Move me, astonish me… delight my eyes and brain: The Vienna Integrated Model of top-down and bottom-up processes in Art Perception (VIMAP) and corresponding affective, evaluative, and neurophysiological correlates. *Phys. Life Rev.* **21**, 80–125 (2017).
14. Jacobsen, T. & Höfel, L. Aesthetics Electrified: An Analysis of Descriptive Symmetry and Evaluative Aesthetic Judgment Processes Using Event-Related Brain Potentials. *Empir. Stud. Arts* **19**, 177–190 (2001).

ACCEPTED MANUSCRIPT

Downloaded from https://academic.oup.com/pnasnexus/advance-article/doi/10.1093/pnasnexus/pgaf288/8249480 by guest on 16 September 2025

15. Jacobsen, T. & Höfel, L. Descriptive and evaluative judgment processes: Behavioral and electrophysiological indices of processing symmetry and aesthetics. *Cogn. Affect. Behav. Neurosci.* **3**, 289–299 (2003).

16. Höfel, L. & Jacobsen, T. Electrophysiological indices of processing aesthetics: Spontaneous or intentional processes? *Int. J. Psychophysiol.* **65**, 20–31 (2007).

17. Jacobsen, T., Schubotz, R. I., Höfel, L. & Cramon, D. Y. v. Brain correlates of aesthetic judgment of beauty. *Neuroimage* **29**, 276–285 (2006).

18. Brattico, E., Jacobsen, T., De Baene, W., Glerean, E. & Tervaniemi, M. Cognitive vs. affective listening modes and judgments of music–An ERP study. *Biol. Psychol.* **85**, 393–409 (2010).

19. Wang, D., Weisstein, F. L., Duan, S. & Choi, P. Impact of ambivalent attitudes on green purchase intentions: The role of negative moods. *Int. J. Consum. Stud.* **46**, 182–199 (2022).

20. Bertamini, M., Rampone, G., Makin, A. D. & Jessop, A. Symmetry preference in shapes, faces, flowers and landscapes. *PeerJ* **7**, e7078 (2019).

21. Yue, X., Robert, S. & Ungerleider, L. G. Curvature processing in human visual cortical areas. *NeuroImage* **222**, 117295 (2020).

22. Walther, D. B., Farzanfar, D., Han, S. & Rezanejad, M. The mid-level vision toolbox for computing structural properties of real-world images. *Front. Comput. Sci.* **5**, 1140723 (2023).

23. Haegens, S., Luther, L. & Jensen, O. Somatosensory anticipatory alpha activity increases to suppress distracting input. *J. Cogn. Neurosci.* **24**, 677–685 (2012).

24. Sarasso, P. *et al.* Aesthetic appreciation of musical intervals enhances behavioural and neurophysiological indexes of attentional engagement and motor inhibition. *Sci. Rep.* **9**, 18550 (2019).

ACCEPTED MANUSCRIPT

Downloaded from https://academic.oup.com/pnasnexus/advance-article/doi/10.1093/pnasnexus/pgaf288/8249480 by guest on 16 September 2025

25. Bottari, D. *et al.* EEG frequency-tagging demonstrates increased left hemispheric involvement and crossmodal plasticity for face processing in congenitally deaf signers. *Neuroimage* **223**, 117315 (2020).

26. Stropahl, M., Bauer, A.-K. R., Debener, S. & Bleichner, M. G. Source-modeling auditory processes of EEG data using EEGLAB and brainstorm. *Front. Neurosci.* **12**, 309 (2018).

27. Delorme, A. & Makeig, S. EEGLAB: an open source toolbox for analysis of single-trial EEG dynamics including independent component analysis. *J. Neurosci. Methods* **134**, 9–21 (2004).

28. Jung, T.-P. *et al.* Removing electroencephalographic artifacts by blind source separation. *Psychophysiology* **37**, 163–178 (2000).

29. Bell, A. J. & Sejnowski, T. J. An information-maximization approach to blind separation and blind deconvolution. *Neural Comput.* **7**, 1129–1159 (1995).

30. Jung, T.-P. *et al.* Removal of eye activity artifacts from visual event-related potentials in normal and clinical subjects. *Clin. Neurophysiol.* **111**, 1745–1758 (2000).

31. Widmann, A., Schröger, E. & Maess, B. Digital filter design for electrophysiological data–a practical approach. *J. Neurosci. Methods* **250**, 34–46 (2015).

32. Klug, M. & Kloosterman, N. A. Zapline-plus: A Zapline extension for automatic and adaptive removal of frequency-specific noise artifacts in M/ EEG. *Hum. Brain Mapp.* **43**, 2743–2758 (2022).

33. de Cheveigné, A. ZapLine: A simple and effective method to remove power line artifacts. *NeuroImage* **207**, 116356 (2020).

34. Lalor, E. C., Power, A. J., Reilly, R. B. & Foxe, J. J. Resolving Precise Temporal Processing Properties of the Auditory System Using Continuous Stimuli. *J. Neurophysiol.* **102**, 349–359 (2009).

35. Oostenveld, R., Fries, P., Maris, E. & Schoffelen, J.-M. FieldTrip: Open Source Software for Advanced Analysis of MEG, EEG, and Invasive Electrophysiological Data. *Comput. Intell. Neurosci.* **2011**, 1–9 (2011).

ACCEPTED MANUSCRIPT

Downloaded from https://academic.oup.com/pnasnexus/advance-article/doi/10.1093/pnasnexus/pgaf288/8249480 by guest on 16 September 2025

36. Urbach, T. P. & Kutas, M. The intractability of scaling scalp distributions to infer neuroelectric sources. *Psychophysiology* **39**, 791–808 (2002).

37. Tallon-Baudry, C. & Bertrand, O. Oscillatory gamma activity in humans and its role in object representation. *Trends Cogn. Sci.* **3**, 151–162 (1999).

38. Siegel, M., Donner, T. H. & Engel, A. K. Spectral fingerprints of large-scale neuronal interactions. *Nat. Rev. Neurosci.* **13**, 121–134 (2012).

39. Maris, E. & Oostenveld, R. Nonparametric statistical testing of EEG- and MEG-data. *J. Neurosci. Methods* **164**, 177–190 (2007).

40. Chuquichambi, E. G. *et al.* How universal is preference for visual curvature? A systematic review and meta-analysis. *Ann. N. Y. Acad. Sci.* **1518**, 151–165 (2022).

41. Barne, L. C., de Lange, F. P. & Cravo, A. M. Prestimulus alpha power is related to the strength of stimulus representation. *Cortex* **132**, 250–257 (2020).

42. Di Russo, F. *et al.* Beyond the "Bereitschaftspotential": Action preparation behind cognitive functions. *Neurosci. Biobehav. Rev.* **78**, 57–81 (2017).

43. Raś, M., Nowik, A., Klawiter, A. & Króliczak, G. When is the brain ready for mental actions? Readiness potential for mental calculations. *Acta Neurobiol. Exp. (Warsz.)* **79**, 386–398 (2019).

44. Byrne, A. *et al.* Investigating the effect of losses and gains on effortful engagement during an incentivized Go/NoGo task through anticipatory cortical oscillatory changes. *Psychophysiology* **59**, e13897 (2022).

45. Alexander, P. *et al.* Readiness potentials driven by non-motoric processes. *Conscious. Cogn.* **39**, 38–47 (2016).

46. Capotosto, P., Babiloni, C., Romani, G. L. & Corbetta, M. Frontoparietal cortex controls spatial attention through modulation of anticipatory alpha rhythms. *J. Neurosci.* **29**, 5863–5872 (2009).

ACCEPTED MANUSCRIPT

Downloaded from https://academic.oup.com/pnasnexus/advance-article/doi/10.1093/pnasnexus/pgaf288/8249480 by guest on 16 September 2025

47. Liu, Y., Huang, H., McGinnis-Deweese, M., Keil, A. & Ding, M. Neural substrate of the late positive potential in emotional processing. *J. Neurosci.* **32**, 14563–14572 (2012).

48. Deng, X., Sang, B., Ku, Y. & Sai, L. Age-related differences in the late positive potential during emotion regulation between adolescents and adults. *Sci. Rep.* **9**, 5738 (2019).

49. Hajcak, G., Dunning, J. P. & Foti, D. Motivated and controlled attention to emotion: time-course of the late positive potential. *Clin. Neurophysiol.* **120**, 505–510 (2009).

50. Hajcak, G., MacNamara, A., Foti, D., Ferri, J. & Keil, A. The dynamic allocation of attention to emotion: Simultaneous and independent evidence from the late positive potential and steady state visual evoked potentials. *Biol. Psychol.* **92**, 447–455 (2013).

51. Mocaiber, I. *et al.* Fact or fiction? An event-related potential study of implicit emotion regulation. *Neurosci. Lett.* **476**, 84–88 (2010).

52. Meynadasy, M. A. *et al.* Emotion regulation and the late positive potential (LPP) in older adults. *Int. J. Psychophysiol.* **177**, 202–212 (2022).

53. Dennis, T. A. & Hajcak, G. The late positive potential: a neurophysiological marker for emotion regulation in children. *J. Child Psychol. Psychiatry* **50**, 1373–1383 (2009).

54. Foti, D. & Hajcak, G. Deconstructing reappraisal: descriptions preceding arousing pictures modulate the subsequent neural response. *J. Cogn. Neurosci.* **20**, 977–988 (2008).

55. Sarasso, P. *et al.* Preferred music listening is associated with perceptual learning enhancement at the expense of self-focused attention. *Psychon. Bull. Rev.* 1–14 (2022).

56. Jaušovec, N., Jaušovec, K. & Gerlič, I. The influence of Mozart's music on brain activity in the process of learning. *Clin. Neurophysiol.* **117**, 2703–2714 (2006).

57. Barbieri, P. *et al.* The aesthetic valve: how aesthetic appreciation may switch emotional states from anxiety to curiosity. *Philos. Trans. R. Soc. B Biol. Sci.* **379**, 20220413 (2024).

ACCEPTED MANUSCRIPT

Downloaded from https://academic.oup.com/pnasnexus/advance-article/doi/10.1093/pnasnexus/pgaf288/8249480 by guest on 16 September 2025

58. Schmidhuber, J. Formal theory of creativity, fun, and intrinsic motivation (1990–2010). *IEEE Trans. Auton. Ment. Dev.* **2**, 230–247 (2010).

59. Brielmann, A. A. & Dayan, P. A computational model of aesthetic value. *Psychol. Rev.* (2022).

60. Van De Cruys, S., Frascaroli, J. & Friston, K. Order and change in art: towards an active inference account of aesthetic experience. *Philos. Trans. R. Soc. B Biol. Sci.* **379**, 20220411 (2024).

61. Sarasso, P. *et al.* Nice and easy: Mismatch negativity responses reveal a significant correlation between aesthetic appreciation and perceptual learning. *J. Exp. Psychol. Gen.* **151**, 1433 (2022).

62. Pizzolante, M. *et al.* Aesthetic experiences and their transformative power: a systematic review. *Front. Psychol.* **15**, 1328449 (2024).

63. Sarasso, P. *et al.* Beauty and uncertainty as transformative factors: A free energy principle account of aesthetic diagnosis and intervention in gestalt psychotherapy. *Front. Hum. Neurosci.* (2022).

64. Sarasso, P., Francesetti, G. & Schoeller, F. Possible applications of neuroaesthetics to normal and pathological behaviour. *Front. Neurosci.* **17**, (2023).

65. Sarasso, P., Ronga, I., Neppi-Modona, M. & Sacco, K. The role of musical aesthetic emotions in social adaptation to the Covid-19 pandemic. *Front. Psychol.* **12**, 611639 (2021).

66. Willenbockel, V. *et al.* Controlling low-level image properties: The SHINE toolbox. *Behav. Res. Methods* **42**, 671–684 (2010).

67. Wang, D. *et al.* Metric-based meta-learning model for few-shot fault diagnosis under multiple limited data conditions. *Mech. Syst. Signal Process.* **155**, 107510 (2021).

68. Delorme, A., Sejnowski, T. & Makeig, S. Enhanced detection of artifacts in EEG data using higher-order statistics and independent component analysis. *Neuroimage* **34**, 1443–1449 (2007).

ACCEPTED MANUSCRIPT

Downloaded from https://academic.oup.com/pnasnexus/advance-article/doi/10.1093/pnasnexus/pgaf288/8249480 by guest on 16 September 2025

69. Artoni, F., Delorme, A. & Makeig, S. Applying dimension reduction to EEG data by Principal Component Analysis reduces the quality of its subsequent Independent Component decomposition. *NeuroImage* **175**, 176–187 (2018).

70. Viola, F. C. *et al.* Semi-automatic identification of independent components representing EEG artifact. *Clin. Neurophysiol.* **120**, 868–877 (2009).

71. Pion-Tonachini, L., Kreutz-Delgado, K. & Makeig, S. ICLabel: An automated electroencephalographic independent component classifier, dataset, and website. *NeuroImage* **198**, 181–197 (2019).

72. Skrandies, W. Global field power and topographic similarity. *Brain Topogr.* **3**, 137–141 (1990).

73. Bousquet, O., Boucheron, S. & Lugosi, G. Introduction to Statistical Learning Theory. Lect. Notes Artif. Intell. 3176, 169–207 (2004). - Google Search. https://www.google.com/search?q=Bousquet%2C+O.%2C+Boucheron%2C+S.+%26+Lugosi%2C+G.+Introduction+to+Statistical+Learning+Theory.+Lect.+Notes+Artif.+Intell.+3176%2C+169%E2%80%93207+(2004).&rlz=1C1VDKB_itIT1028IT1028&oq=Bousquet%2C+O.%2C+Boucheron%2C+S.+%26+Lugosi%2C+G.+Introduction+to+Statistical+Learning+Theory.+Lect.+Notes+Artif.+Intell.+3176%2C+169%E2%80%93207+(2004).&gs_lcrp=EgZjaHJvbWUyBggAEEUYOTIGCAEQRRg8MgYIAhBFGDzSAQkxNTI0ajBqMTWoAgCwAgA&sourceid=chrome&ie=UTF-8.

74. ŞahiN, M. & Aybek, E. Jamovi: An Easy to Use Statistical Software for the Social Scientists. *Int. J. Assess. Tools Educ.* **6**, 670–692 (2020).

ACCEPTED MANUSCRIPT

Downloaded from https://academic.oup.com/pnasnexus/advance-article/doi/10.1093/pnasnexus/pgaf288/8249480 by guest on 16 September 2025

Figure Captions

Figure 1. Experimental questions and summary of the main results.

Figure 2A. Stimuli. Images (a) and (b) are two examples of a stimulus category with a different *B* exponent value: (a) *B*=1, (b) *B*=2.5. Images (c) are three examples of photographs (Experiment 2) with homogenized color spectrum, dimension, resolution, luminance, contrast and light reflection.

Figure 2B. Experimental procedures, hypotheses and analyses. The top panel depicts the experimental procedures (the analysis plan is described in Table 1).

Figure 3. Results in the time domain (VEP). Experiment 1 (left panel) and Experiment 2 (right panel). Grand average VEP waveforms (N = 36) elicited by aesthetic (green) and pragmatic (grey) evaluation of synthetic stimuli are depicted in the figure. The green and grey shadow along the waveforms signals the standard error (SE). The waveforms showed early components within the first 200 ms time window (C1 and N170), followed by a LPP emerging around 300 ms. Scalp-maps topographies represent average amplitudes across aesthetic and pragmatic conditions within four time windows. The grey-shaded areas outlined in different colours indicate significant clusters that survived cluster-based permutation correction. The scalp maps display the *t*-value distribution within these significant clusters. The scalp maps outlined in the box with matching colours display the t-value distributions of the effect and the coordinate layout above marks all significant electrodes (coloured dots) that survived the comparison.

Figure 4. Results in the time-frequency domain. Experiment 1 (top panels) and Experiment 2 (bottom panels). Top images of each panel (A, B, D, E) show the time-frequency spectrogram obtained by subtracting the average spectrogram of the pragmatic task from that obtained from the aesthetic task, averaged across all significant channels. Panels A and D illustrate pre-stimulus TFR activity (-1 - 0 s). Panels B and E represent the post-stimulus TFR results (0 - 1 s), with the estimated event-related synchronization (ERS) and desynchronization (ERD). Panels C and F display the results of the pre-stimulus statistical analysis (no significant clusters were detected in the post-stimulus window). These plots show the p_{clust} value mask, indicating the frequency-bands and the temporal intervals where significant differences in power emerged between aesthetic and pragmatic conditions. Colour intensity (i.e., in our case blue, indicating lower power in the aesthetic condition) reflects higher average p-values

ACCEPTED MANUSCRIPT

Downloaded from https://academic.oup.com/pnasnexus/advance-article/doi/10.1093/pnasnexus/pgaf288/8249480 by guest on 16 September 2025

and greater consistency of significant temporal and frequency clusters across channels. The red and green boxes alongside the significant cluster plot showed the average p-value topography of respectively beta and alpha frequencies, extracted in the time and frequency interval signaled from the box with matching colour.

Figure 5: Results of the SVM classifier. Boxes represent interquartile ranges, the horizontal segments the medians, whiskers are min-to-max ranges after outliers removal, and dots refer to single subjects.

Tables

Hypotheses	Analysis Plan	Interpretation given to different outcomes
(1) Images presented during the aesthetic task will trigger decreased pre-stimulus inhibitory alpha power and increased post-stimulus alpha ERD, as well as larger VEPs within the first 200 ms post- stimulus onset, compared to images presented during the pragmatic task.	To investigate the effects of the evaluation task (aesthetic vs. pragmatic), we will employ a cluster-based permutation approach. Single subjects' pre-processed EEG signals averaged across trials will be fed into group-level point-by-point t-tests evidencing clusters that contain voltage amplitude or power that significantly differ across conditions at specific latencies, channels, and/or frequency ranges.	Larger early components of VEPs and alpha ERD during the aesthetic task as compared to pragmatic task will be interpreted as the electrophysiological correlates of attentional enhancement during an aesthetic experience. Otherwise, if such indexes will not differ significantly, the attentional enhancement hypothesis should be discarded.
(2) By training a classifier to distinguish between aesthetic and pragmatic judgements on Experiment 1, we should be able to predict the nature of the task	A linear binary classifier will be trained to distinguish between the two tasks, based on four features: power of pre-stimulus alpha, post stimulus alpha ERD, and amplitude of early waves of	The prediction of the type of evaluation (aesthetic vs pragmatic) performed on natural and synthetic images, based on electrophysiological signals, will be interpreted as a further

ACCEPTED MANUSCRIPT

Downloaded from https://academic.oup.com/pnasnexus/advance-article/doi/10.1093/pnasnexus/pgaf288/8249480 by guest on 16 September 2025

based on EEG data from Experiment 2.	the VEPs, also using a bound on the misclassification probability coming from statistical learning theory.	confirmation of the different nature of the tasks and of the electrophysiological pathways involved. If otherwise the nature of the task cannot be predicted based on EEG signal, hypothesis 2 should be discarded.

Table 1. Hypotheses and analysis plan. The hypotheses, the analysis plan and the interpretations proposed for different possible outcomes are presented in the table.

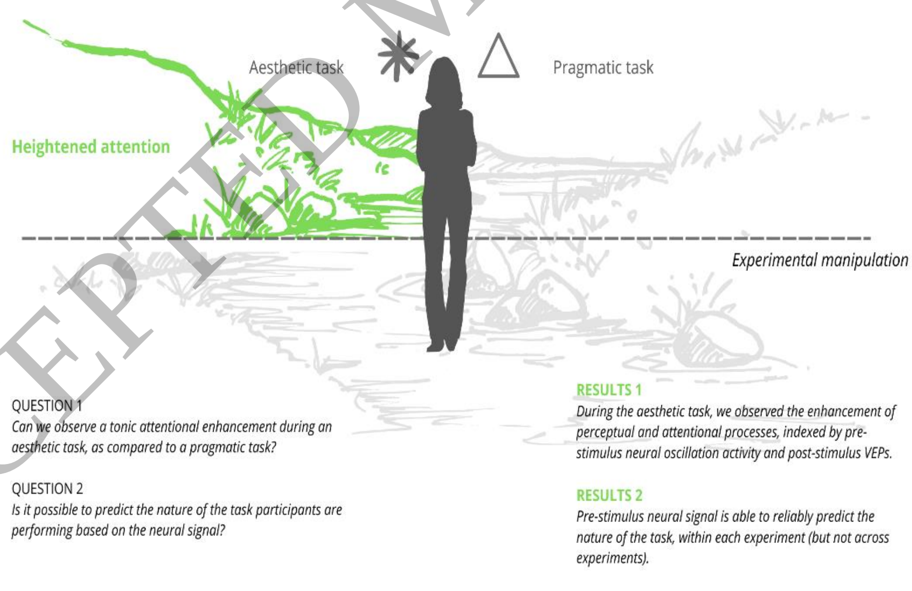

Figure 1

508x286 mm (x DPI)

ACCEPTED MANUSCRIPT

Downloaded from https://academic.oup.com/pnasnexus/advance-article/doi/10.1093/pnasnexus/pgaf288/8249480 by guest on 16 September 2025

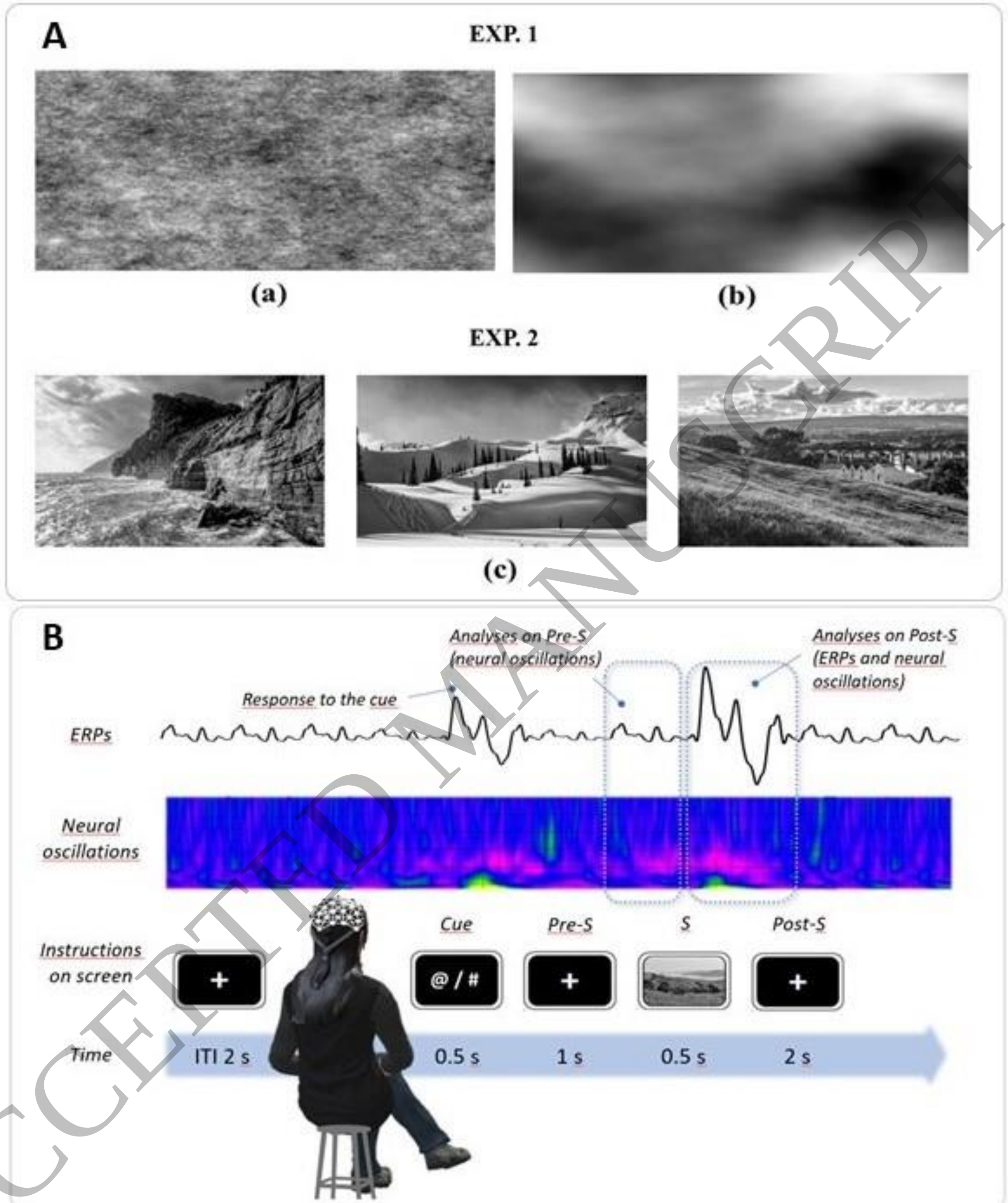

Figure 2

155x188 mm (x DPI)

ACCEPTED MANUSCRIPT

Downloaded from https://academic.oup.com/pnasnexus/advance-article/doi/10.1093/pnasnexus/pgaf288/8249480 by guest on 16 September 2025

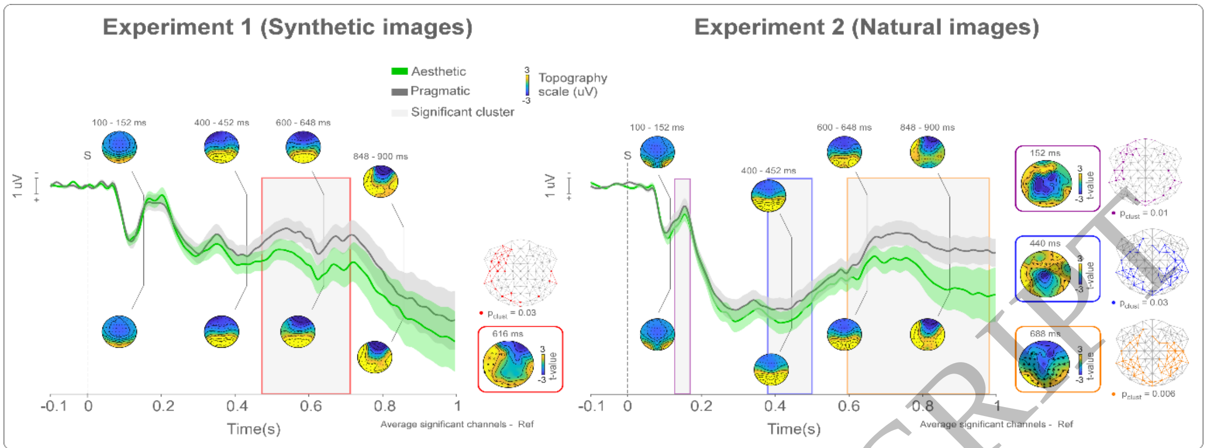

Figure 3

559x225 mm (x DPI)

ACCEPTED MANUSCRIPT

Downloaded from https://academic.oup.com/pnasnexus/advance-article/doi/10.1093/pnasnexus/pgaf288/8249480 by guest on 16 September 2025

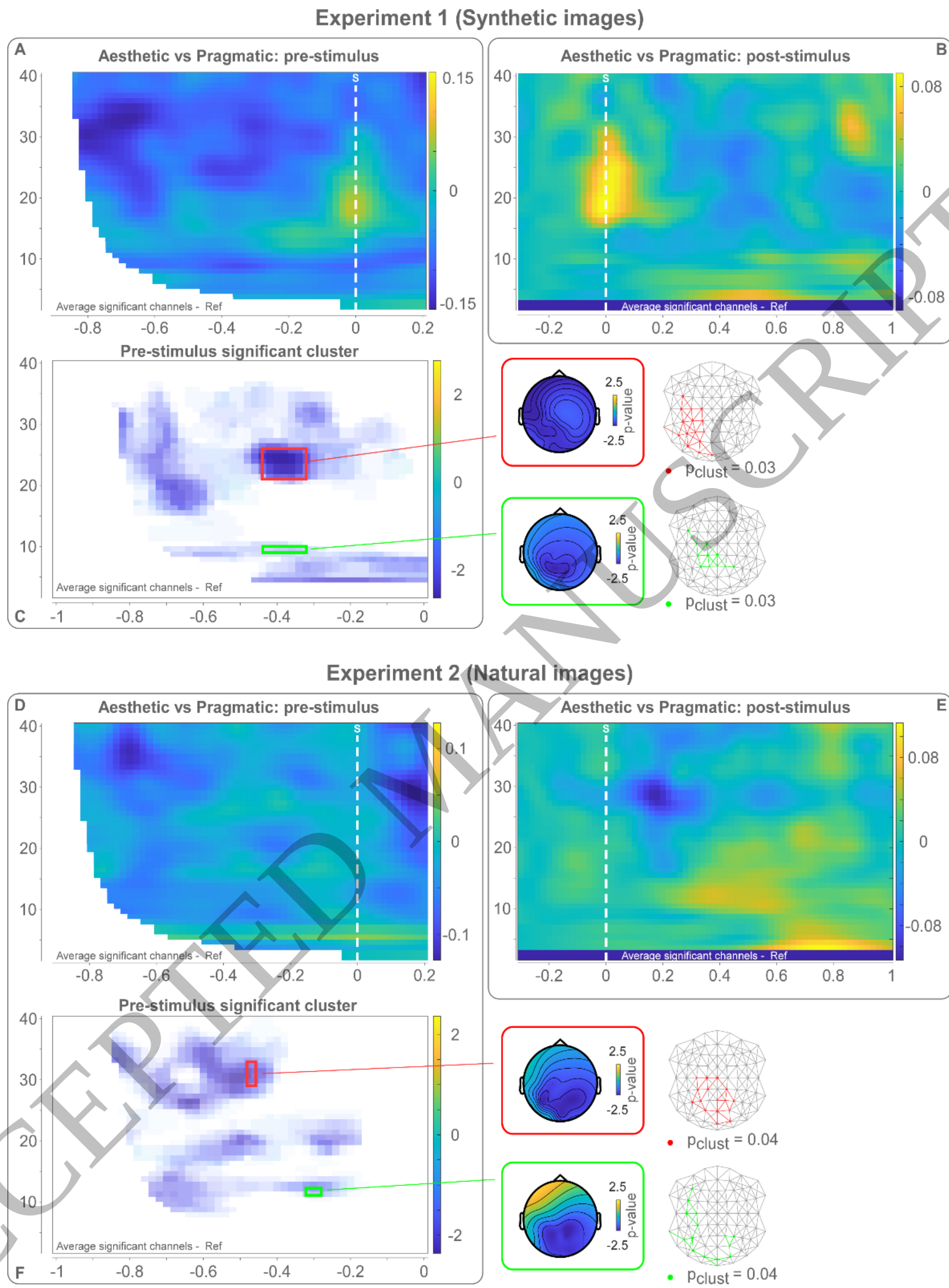

Figure 4

376x491 mm (x DPI)

ACCEPTED MANUSCRIPT

Downloaded from https://academic.oup.com/pnasnexus/advance-article/doi/10.1093/pnasnexus/pgaf288/8249480 by guest on 16 September 2025

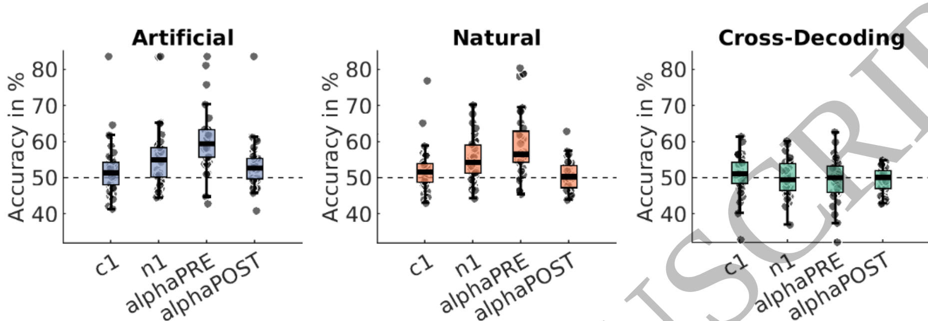

1

2 **Figure 5**

3 **148x111 mm (x DPI)**

ACCEPTED MANUSCRIPT

Downloaded from https://academic.oup.com/pnasnexus/advance-article/doi/10.1093/pnasnexus/pgaf288/8249480 by guest on 16 September 2025